Understanding dynamics of *Plasmodium falciparum* gametocytes production: Insights from an age-structured model

Ramsès Djidjou-Demasse[a,*], Arnaud Ducrot[b], Nicole Mideo[c], Gaëtan Texier[d,e]

[a] MIVEGEC, Univ. Montpellier, IRD, CNRS, Montpellier, France

[b] Normandie Univ., UNIHAVRE, LMAH, FR-CNRS-3335, ISCN, 76600 Le Havre, France

[c] Department of Ecology & Evolutionary Biology, University of Toronto, Toronto, Canada

[d] Aix Marseille Univ., IRD, AP-HM, SSA, VITROME, IHU Méditerranée Infection, Marseille, France

[e] Centre d'Epidémiologie et de Santé Publique des Armées (CESPA), Marseille, France.

[*] Author for correspondence: ramses.djidjoudemasse@ird.fr

Abstract

Many models of within-host malaria infection dynamics have been formulated since the pioneering work of Anderson *et al.* in 1989. Biologically, the goal of these models is to understand what governs the severity of infections, the patterns of infectiousness, and the variation thereof across individual hosts. Mathematically, these models are based on dynamical systems, with standard approaches ranging from K-compartments ordinary differential equations (ODEs) to delay differential equations (DDEs), to capture the relatively constant duration of replication and bursting once a parasite infects a host red blood cell. Using malariatherapy data, which offers fine-scale resolution on the dynamics of infection across a number of individual hosts, we compare the fit and robustness of one of these standard approaches (K-compartments ODEs) with a partial differential equations (PDEs) model, which explicitly tracks the "age" of an infected cell. We found that a PDE model outperforms the K-compartments ODEs, in terms of robustness in representing the observed gametocyte dynamics where the number K of repeated compartments for the goodness-of-fit is quite variable across individuals. While both models perform quite similarly in terms of goodness-of-fit for gametocyte production when the initial production of gametocytes is very slow, the K-compartments ODEs model particularly overestimate parasite densities early on in infections. Moreover, while a particular number K of repeated compartments in the ODE model is useful to slow down the initial production of gametocytes, the predicted parasitemia is quite unrealistic when $K \geq 2$. Finally, the PDE model highlights a strong qualitative connection between the density of transmissible parasite stages (*i.e.*, gametocytes) and the density of host-damaging (and asexually-replicating) parasite stages, which is difficult to capture by the K-compartments ODEs model. This finding provides a simple tool for predicting which hosts are most infectious to mosquitoes —vectors of *Plasmodium* parasites— which is a crucial component of global efforts to control and eliminate malaria.

Key words. Within-host model, malaria, gametocytemia, parasitemia, infectiousness

1 Introduction

Malaria has always been a public health problem and, since the discovery of malaria parasites in human blood by Charles Laveran in 1880, remains so despite more than 100 years of research. Malaria continues to have a significant impact on the world with over 400,000 deaths alone each year [54]. It is a vector-borne disease caused by five plasmodial species: *Plasmodium falciparum, P. vivax, P. malariae, P. ovale, and P. knowlesi*, with *P. falciparum* being the most pathogenic species infecting humans [35].

The malaria parasite has a complex life cycle involving sexual reproduction occurring in the insect vector [2] and two stages of infection within a human (or animal host), a liver stage [24] and blood stage [6]. Human infection starts by the bite of an infected mosquito, which injects the sporozoite form of *Plasmodium* during a blood meal. The sporozoites enter the host peripheral circulation, and rapidly transit to the liver where they infect liver cells (hepatocytes) [24]. The parasite replicates within the liver cell before rupturing to release extracellular parasite forms (merozoites), into the host circulation, where they may invade red blood cells (RBCs) to initiate blood stage infection [43]. Then follows a series of cycles of replication, rupture, and re-invasion of the RBC. Some asexual parasite forms commit to an alternative developmental pathway and become sexual forms (gametocytes) [47]. Gametocytes can be taken up by mosquitoes during a blood meal where they undergo a cycle of sexual development to produce sporozoites [2], which completes the parasite life cycle.

The classical model of within-host parasite multiplication in malaria infections was formulated by Anderson *el al.* [4]. This model tracks uninfected red blood cells (RBCs), parasitized RBCs (pRBCs) and merozoites. The pioneer work of Anderson *el al.* [4], has been further developed in several directions including in particular immune response, see for instance [1, 25, 28–30, 36, 44, 45] for human malaria infection. We also mention discrete-time models such as in [18]. Those models use an exponential process to describe the rate of rupture of pRBCs and, as a consequence, then fail to capture realistic lifetimes of the pRBCs on short time scales [49]. One reason for this is that they are essentially Markovian, *i.e.* 'memoryless', a RBC that has been parasitized for 40 hours has the same probability of producing merozoites as *e.g.* a RBC parasitized less than a hour ago. Moreover, those models are treating some processes that are likely to be kinda continuous as occurring only in a narrow window (*e.g.*, the development of parasites within RBCs and the rupture of pRBC followed by the merozoites release phenomenon).

To correct this issue, some models of malaria infection include K-compartments ordinary differential equations (ODEs) representing a progression through a parasite's developmental cycle, *e.g.* [25, 32, 48, 55], or delay differential equations (DDEs) to capture the time pRBCs take to mature before producing new merozoites, *e.g.* [11, 30, 34, 40]. Other approaches are the use of partial differential equations (PDEs) to track the age-structure of the pRBC population [5, 16, 17, 35]. It is shown in [23] that DDEs perform better than the ODEs in representing the dynamics of red blood cells during malaria infection.

The K-compartments ODEs model can be interpreted as the application of the method of stages (or the "linear chain trick") to the life cycle of pRBC, *e.g.* see [22, 31, 32] and references therein. One problem with the K-compartments ODEs model is how to decide

upon the number of repeated compartments to capture the realistic dynamics of the pRBCs [26]. Determining the distribution of mean waiting times across compartments for the ODE model is also an issue. If the compartments can be considered equivalent to the developmental stages of pRBCs, then parasites might not spend equal time in each stage.

We first introduce both mathematical models (PDE and K-compartments ODEs) and define the model's parameters and outputs. Next, using gametocyte production as a proxy variable of infectiousness, we compared the model outputs from a PDE stage-structured formulation to those from classical K-compartments ODEs. Furthermore, the output of both mathematical models is used to qualitatively recover the time course of parasitemia, defined as the proportion of all infected RBCs among the total number of RBCs. Finally, the PDE model is used to highlight a strong qualitative connection between gametocyte density and parasitemia, which is difficult to capture by the K-compartments ODEs model.

2 Material and method

2.1 Data and methodology

Our analysis is based on data collected from malariatherapy taken in [21]. Malaria inoculation was a recommended treatment for neurosyphilis between 1940 and 1963. We also refer to [12] for a review paper on malariatherapy and the knowledge gained in the understanding of malaria infection. The data we shall use consist in daily records of gametocyte density for twelve patients. Although malariatherapy has been dismissed for obvious ethical reasons, the advantages to use such data are multiple. Indeed, patients are naive to malaria infection and the dynamics are not perturbed by anti-malarial treatments. Let us notice that such data have been widely used in the literature and in particular to estimate mathematical model parameters. We refer to [21] and the references therein.

The method we shall develop consists in devising a mathematical model to describe the intra-host development of the infection and fitting the model to the available data. The output of the mathematical model will allow us to access various quantities related to the time course of the infection, including parasitemia.

2.2 Mathematical model

As discussed above, we now present the mathematical model we shall use to recover parasitemia for twelve patients from observed time courses of gametocyte density. We shall describe the within-host malaria infection coupled with red blood cells (RBCs) production as well as immune effectors. Fig. 1 presents the flow diagram of the model considered in this note. Our model is divided into four parts: (i) uninfected RBC (uRBCs) dynamics; (ii) changes in parasite stage or parasite maturity; (iii) Gametocyte production and dynamics and (iv) immune response dynamics.

For uRBCs dynamics, we divide cells into three age classes: reticulocyte (young), mature and senescent. All three ages are vulnerable to *P. falciparum* infection. This can be different for other species of *Plasmodium*. Although we focus in this work on the case of *P. falciparum*, the model described below could be applied to study other species

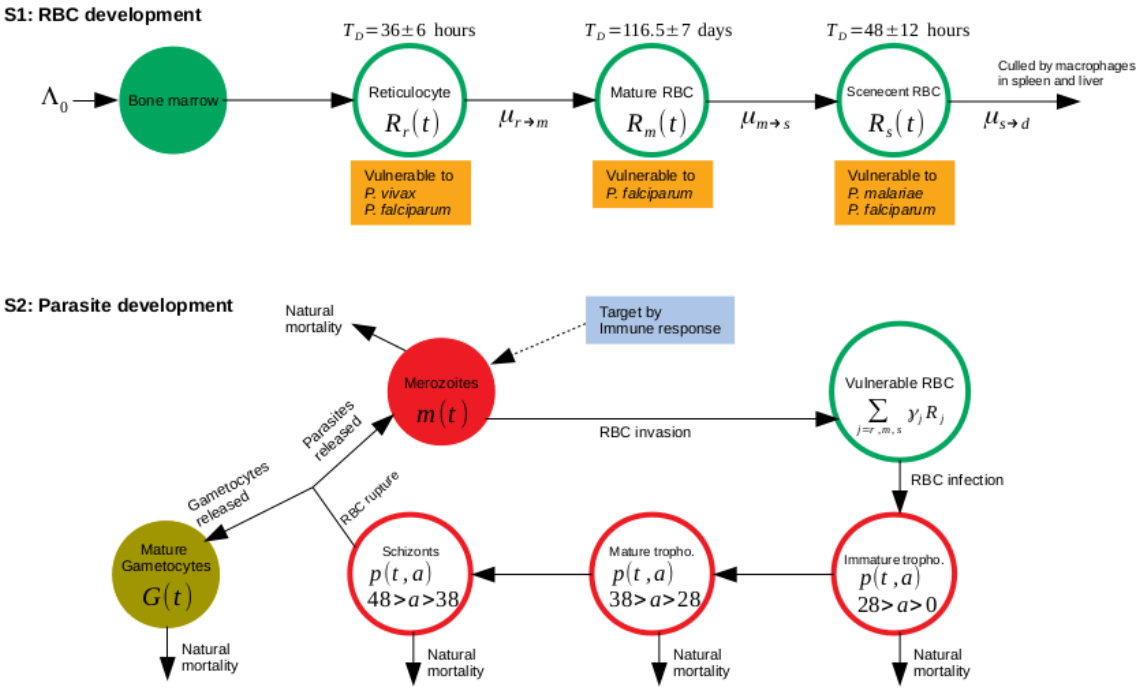

Figure 1: (S_1) The RBC development chain, (S_2) the parasite development chain. T_D= average duration (± one standard deviation) spent in an RBC age class given in [42], Λ_0 is the RBC production rate from the marrow source. In our model, the parameter $1/\mu_{r\to m}$ (resp. $1/\mu_{m\to s}$, $1/\mu_{s\to d}$) is the time spent in RBC reticulocyte (resp. mature, senescent) class. A continuous parameter a denotes the time since the concerned RBC is parasitized: ring stage ($0 < a < 26$ hours), trophozoite ($26 < a < 38$ hours) and schizont ($38 < a < 48$ hours). In the case of *P. falciparum* infection, one has ($\gamma_r = \gamma_m = \gamma_s = 1$) while for *P. vivax* one has ($\gamma_r = 1$, $\gamma_m = \gamma_s = 0$) and for *P. malariae* ($\gamma_r = \gamma_m = 0$, $\gamma_s = 1$) [46].

such as *P. vivax* or *P. malariae*, which have specific RBC-age preferences [46]. Such age-structured dynamics for uRBC are well known in the literature, see for instance [41]. For the parasites, we consider stage-structured dynamics for their development within pRBC. Here the stage is a continuous variable representing the time since the concerned RBC is parasitized. Such a continuous stage structure will allow us to track the development of parasites within RBCs, but also to have a refined description of the pRBC rupture and of the merozoites release phenomenon. We also emphasize that such a model easily allows for inclusion of anti-malarial treatments acting on only some parasite developmental stages.

Uninfected RBC dynamics. We denote by $R_r(t)$, $R_m(t)$ and $R_s(t)$ respectively the density of reticulocytes, mature RBCs and senescent RBCs at time t.

In the absence of malaria parasites, the evolution of circulating red blood cells is assumed to follow a discrete age maturation system of ordinary differential equations that take the form

$$\begin{cases} \frac{dR_r(t)}{dt} = \Lambda_0 - \mu_{r\to m} R_r(t), \\ \frac{dR_m(t)}{dt} = \mu_{r\to m} R_r(t) - \mu_{m\to s} R_m(t), \\ \frac{dR_s(t)}{dt} = \mu_{m\to s} R_m(t) - \mu_{s\to d} R_s(t). \end{cases} \tag{1}$$

The parameters $1/\mu_{r\to m}$, $1/\mu_{m\to s}$ and $1/\mu_{s\to d}$ respectively denote the average duration of RBCs in the reticulocyte, mature and senescent age classes while Λ_0 represents the normal value of the RBC production from marrow source (i.e. the production rate of RBC). System (1) can also be found in [41].

The parameters of this system are selected from [29, 41] (see Table 1) so that in the absence of parasites, the equilibrium age distribution is given by

$$(R_r^*; R_m^*; R_s^*) = (62.50; 4853; 83.30) \times 10^6 \text{ cell/ml}. \tag{2}$$

This leads to the homeostatic equilibrium concentration of RBC ($R_r^* + R_m^* + R_s^*$) around 4.99×10^9 cells/ml which is in the range expected for humans.

Parasite dynamics with stage-structured formulation (PDE model). Here we consider the interaction between free merozoites together with the circulating RBCs. We, respectively, denote by $m(t)$, $p(t,a)$ and $G(t)$ the density of merozoites, parasitized RBC, and mature gametocytes at time t. The variable a denotes the time since the concerned RBC is parasitized (i.e. $\int_{a_1}^{a_2} p(t,a)da$ corresponds to the density of pRBC at time t which are infected since the time $a_1 < a < a_2$). The system we shall consider reads as:

$$\begin{cases} p(t,0) = \beta m(t) \sum\limits_{j=r,m,s} \gamma_j R_j(t), \\ \partial_t p(t,a) + \partial_a p(t,a) = -\left(\mu(a) + d_0\right) p(t,a), \\ \dot{m}(t) = (1-\alpha_G) \int_0^\infty r\mu(a) p(t,a) da - \mu_m m(t) - \beta m(t) \sum\limits_{j=r,m,s} \gamma_j R_j(t), \\ \dot{G}(t) = \alpha_G \int_0^\infty r\mu(a) p(t,a) da - \mu_G G(t). \end{cases} \tag{3}$$

We briefly sketch the interpretation of the parameters arising in (3). Parameters d_0, μ_m and μ_G, respectively, denote the natural death rates for uRBC, for free merozoites and for mature gametocytes. Function $\mu(a)$ denotes the additional death rate of pRBC due to the parasites at stage a and leading to the rupture. The rupture of pRBC at stage a results

in the release of an average number r of merozoites into the blood stream, so that pRBC then produce, at stage a, merozoites at rate $r\mu(a)$. Together with this description, the quantity $\int_0^\infty r\mu(a)p(t,a)da$ corresponds to the number of merozoites produced by pRBC at time t. The parameter β describes the contact rate between uRBC and free merozoites. Parameters γ_k with $k = r, m, s$ describe the age preference of parasites' targets. Here we shall be concerned in *P. falciparum* infection that does not have any preference for RBC so that $\gamma_r = \gamma_m = \gamma_s = 1$. However when considering *P. vivax* infection one has $\gamma_r = 1$ and $\gamma_m = \gamma_s = 0$, so that target RBCs mostly consist in reticulocyltes while when *P. malariae* infection is concerned then target RBCs are mostly senescent cells, that is $\gamma_r = \gamma_m = 0$ and $\gamma_s = 1$ [46]. The parameter α_G represents the proportion of merozoites from a bursting asexual schizonts that will enter the gametocyte compartment, *i.e.*, are "committed" to the gametocyte developmental pathway. For simplicity, we have ignored the age structure of gameteocytes and consider G as capturing mature, measurable gametocytes.

Parasite dynamics with K-compartments ODEs formulation (ODE model). For the ODE model formulation, we consider K stages for the pRBC before rupture and set $p = (p_1, p_2, p_3, \cdots, p_K)$, such that $p_j(t)$ denotes the concentration of pRBC at time t. Then, setting $\dot{z} = \frac{\mathrm{dz}}{\mathrm{dt}}$ the ODE model writes

$$\begin{cases} \dot{p}_1(t) = \beta m(t) \sum\limits_{j=r,m,s} \gamma_j R_j(t) - (\mu_1 + d_1)\, p_1(t), \\ \dot{p}_2(t) = \mu_1 p_1(t) - (\mu_2 + d_2)\, p_1(t), \\ \vdots \\ \dot{p}_K(t) = \mu_{K-1} p_{K-1}(t) - (\mu_K + d_K)\, p_K(t), \\ \dot{m}(t) = (1-\alpha_G) r\mu_K p_K(t) - \mu_m m(t) - \beta m(t) \sum\limits_{j=r,m,s} \gamma_j R_j(t), \\ \dot{G}(t) = \alpha_G r\mu_K p_K(t) - \mu_G G(t), \end{cases} \tag{4}$$

wherein $1/\mu_i$ the duration of the i-stage and d_i the death rate of pRBC. The number of stages K is variable and other parameters and state variables are the same as for the PDE model.

The immune responses. Following [18], here we consider two immune responses (IRs) controlling the growth of the parasite population: (i) an innate IR $S_I(t)$ at time t representing the effect of the pro-inflammatory cytokine cascade and (ii) an adaptive IR $S_A(t)$ at time t. The effect of the innate IR is a function of the present parasite (merozoite) density that takes the form

$$S_I(t) = \frac{m(t)}{m(t) + S_I^*}, \tag{5}$$

where S_I^* is the critical parasite density at which the current multiplication factor is reduced by 50%.

The adaptive IR is a function of the cumulative parasite density; this function is determined by two host-specific parameters and one constant: (1) S_A^* is the critical cumulative parasite density at which the current multiplication factor is reduced by 50%; (2) $\Delta_0 = 16$ days is the average delay required by adaptive IR to become effective [18],

i.e., for time t before Δ_0 the cumulative density is set to zero (the adaptive IR has no effect and $S_A(t) = 0$ for $t \leq \Delta_0$) and (3) $\Delta_1 = 8$ days is the delay that determines the last term in the cumulative density for times $t \geq \Delta_0$, i.e.,

$$S_A(t) = \begin{cases} \dfrac{\int_{\Delta_0}^{t} m(s)ds}{\int_{\Delta_0}^{t} m(s)ds + S_A^*}, & \Delta_0 \leq t < \Delta_0 + \Delta_1; \\ \dfrac{\int_{\Delta_0}^{\Delta_0+\Delta_1} m(s)ds}{\int_{\Delta_0}^{\Delta_0+\Delta_1} m(s)ds + S_A^*}, & t \geq \Delta_0 + \Delta_1. \end{cases} \tag{6}$$

Thus, including these two IR effects, the dynamics of asexual parasite concentration $m(t)$ should be replaced in Models (3) and (4) respectively by:

$$\dot{m}(t) = (1-\alpha_G)\int_0^{\infty} r\mu(a)p(t,a)da - \left(\mu_m + \beta \sum_{j=r,m,s} \gamma_j R_j(t) + S_A(t)\right) m(t) - S_I(t), \tag{7}$$

and

$$\dot{m}(t) = (1-\alpha_G)r\mu_K p_K(t) - \left(\mu_m + \beta \sum_{j=r,m,s} \gamma_j R_j(t) + S_A(t)\right) m(t) - S_I(t). \tag{8}$$

Initial conditions. For both PDE and ODE models, the initial RBCs are assumed to be at their homeostatic equilibrium distribution in the absence of parasites given by (2), *i.e.*, $R_r(0) = R_r^*$; $R_m(0) = R_m^*$; $R_s(0) = R_s^*$. The above models are also assumed to be free of pRBCs at the initial time, and the initial density of malaria parasites is such that $m(0) = m_0$, with m_0 a positive constant. These initial conditions are summarized in Table 2.

Parasitemia. The output of both mathematical models can be used to recover the time course of parasitemia, defined as the proportion of all infected RBC among the total number of RBC. Using the notation of the model, the parasitemia at time t, denoted by $P(t)$ is calculated as follows

$$P(t) = \underbrace{\frac{\int_0^{\infty} p(t,a)da}{\int_0^{\infty} p(t,a)da + \sum_{j=r,m,s} R_j(t)}}_{\text{PDE model}} \text{ or } \underbrace{\frac{\sum_{l=1}^{K} p_l(t)}{\sum_{l=1}^{K} p_l(t) + \sum_{j=r,m,s} R_j(t)}}_{\text{ODE model}}. \tag{9}$$

3 Results

3.1 Development of parasites within RBCs and rupture of pRBCs

An important characteristic of *P. falciparum* is the development of parasites within RBCs. The parasite within a RBC then takes an average of 48 hours to mature and release free merozoites.

With a sequential progression through K stages of parasite maturity before the rupture of the pRBC, the ODE model quantifies the average parasite's development period by

$$\frac{1}{\mu_1} + \cdots + \frac{1}{\mu_K} = 48 \text{ hours}, \tag{10}$$

where $1/\mu_i$ is the waiting time across the i-stage of maturity. Indeed, the probability of the pRBC of being in the i-stage after a hours of infection is then given by $D_i(a) = \mathbb{P}(\tau_i > a)$, where τ_i denotes the duration within the i-th compartment. One assumption of the K-compartments ODE model is that variables τ_i,s are independents and exponentially distributed with parameter μ_i (*i.e.* $D_i(a) = e^{-\mu_i a}$, without taking into account other mechanisms such as natural mortality), such that (10) is satisfied. Thus, $\sum_{i=1}^{K} \mathbb{E}[\tau_i] = \sum_{i=1}^{K} 1/\mu_i = 48$ hours.

With the PDE model, the development of parasites within RBCs is characterized by the rupture function $\mu(a)$, which takes the form

$$\mu(a) = \begin{cases} 0 \text{ if } a < 48 \text{ hours}, \\ \overline{\mu} \text{ if } a \geq 48 \text{ hours}, \end{cases}$$

where a is the age of the pRBC and $\overline{\mu}$ is a positive parameter. With such formulation, the overall average development period is ≈ 48 hours as for the ODE model. Indeed, let $D(a) = \exp\left(-\int_0^a \mu(\sigma)d\sigma\right)$ the probability that a pRBC remains parasitized after a hours (without taking into account other mechanisms such as the natural mortality). Then, the average parasite's development period is

$$\int_0^\infty D(a)da = 48 + \frac{1}{\overline{\mu}}.$$

Here we fix, for *e.g.* $\overline{\mu} = 10$, such that $\int_0^\infty D(a)da = 48 + \dfrac{1}{\overline{\mu}} \approx 48$. The value of $\overline{\mu}$ is therefore not strictly significant as soon as the last approximation holds.

Consequently, the PDE model formulation allows to continuously track the development of parasites within RBCs and then to have a refined description of the pRBC rupture followed by the merozoites release phenomenon. By contrast, besides the issue of determining the maturation probability $\{D_i\}_{i=1,\cdots,K}$, such a continuous process is quite difficult to capture with the ODE model with K repeated stages (Fig. 2A).

One option for defining the maturation probability $\{D_i\}_{i=1,\cdots,K}$ can be obtained through a "linear chain trick" formulation. Indeed, by assuming that the duration of each repeated compartments is the same (*i.e.*, $\mu_i = \mu_0$, for all $i = 1, \cdots, K$), by (10), we then have $D_i(a) = e^{-aK/48}$, for all $i = 1, \cdots, K$. The total duration before rupture becomes $T_K = \sum_{i=1}^{K} D_i$. Here D_i,s are independent and identically distributed with exponential law of parameter $\mu_0 = K/48$. Hence, T_K follows a Gamma distribution $\Gamma(K, \mu_0^{-1}) = \Gamma\left(K, \frac{48}{K}\right)$. We recover that the mean value of T_K is $48h$ and also that its variance is given by $\text{var}(T_K) = 48^2/K$. The latter quantity tends to 0 as $K \to \infty$ meaning that $T_K \to 48$ as $K \to \infty$. As a consequence of the above computations, when K is very large the probability that a pRBC remains parasitized after a hours, is approximately given by $\mathbb{P}(T_K \geq a) \approx 1$ if $a \leq 48$ else 0, that is close to $D(a)$ when $\overline{\mu}$ is large.

However, the main problem with such formulation is that the maturation probability D_i,s will be very low as K increases (Fig. 2B-D). As a consequence, this will lead to a

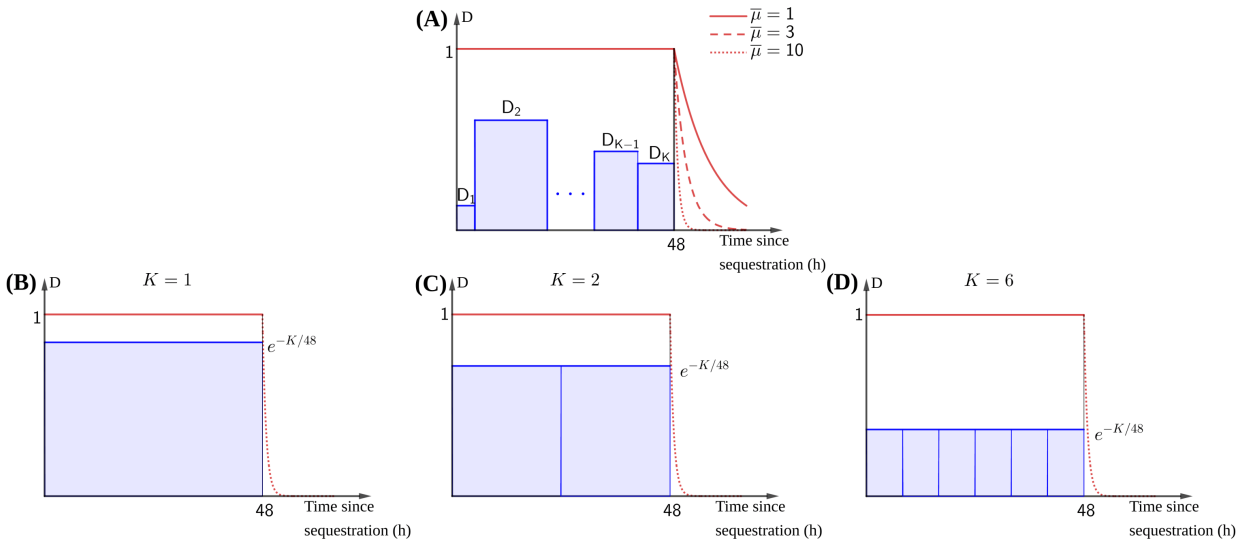

Figure 2: Probability of the pRBC of being in a given stage since parasitation. (A) The maturation probability $\{D_i\}_{i=1,\cdots,K}$ is for the ODE model, while the continuous function D if for the PDE model with different values of $\overline{\mu}$. (B)-(D) With a constant duration of each repeated compartments for $K = 1$, 2 and 6.

wide underestimation of the development of the overall parasite dynamics (see Appendix A for details).

3.2 Within-host reproduction number

The basic reproduction number, usually denoted as $\mathcal{R}_0$, is defined as the total number of parasites arising from one newly pRBC introduced into an uninfected host. It can be used to study the spread of the malaria parasite in an uninfected host, and the parasite will spread if $\mathcal{R}_0 > 1$. The $\mathcal{R}_0$ of the K-compartments ODEs and PDE models write

$$\mathcal{R}_0 = \begin{cases} \dfrac{\beta}{\mu_m + \beta \sum\limits_{j=r,m,s} R_j^*}(1-\alpha_G) r \prod_{i=1}^{K} \dfrac{\mu_i}{\mu_i + d_i} \left(\sum\limits_{j=r,m,s} R_j^* \right), \text{ ODE} \\ \dfrac{\beta}{\mu_m + \beta \sum\limits_{j=r,m,s} R_j^*}(1-\alpha_G) r \dfrac{\overline{\mu}}{\overline{\mu} + d_0} e^{-48 \times d_0} \left(\sum\limits_{j=r,m,s} R_j^* \right), \text{ PDE.} \end{cases} \tag{11}$$

We refer to [17, 32] for details on the derivation of (11).

While the probability for merozoites production for each infection cycle is always 1 for the ODE model, such probability is $\frac{\overline{\mu}}{\overline{\mu}+d_0}$ for the PDE model. One reason for this is that the K-compartments ODEs model is essentially Markovian, *i.e.* 'memoryless'. With the K-compartments ODEs model, a RBC that has been parasitized for 40 hours has the same probability of producing merozoites as *e.g.* a RBC parasitized less than a hour ago.

However, parameter $\overline{\mu}$ can then be chosen such that these probabilities are close to unity. For instance, for the PDE model, $\frac{\overline{\mu}}{\overline{\mu}+d_0} \approx 1$ as soon as $\overline{\mu}$ is sufficiently large compared to d_0. Therefore, with the value of $\overline{\mu} = 10$ introduced in the previous section, we have $\frac{\overline{\mu}}{\overline{\mu}+d_0} \approx 0.99$.

Finally, one of the main differences between the $\mathcal{R}_0$ expressions of both models is the probability at which pRBCs survive the 48 hours of the parasite's development period for each infection cycle. While such probability is quantified by the term $e^{-48\times d_0}$ for the PDE model (11), it is $\prod_{i=1}^{K} \frac{\mu_i}{\mu_i+d_i}$ for the ODE model (11). However, in some configurations of parameters μ_i,s and for K sufficiently large we can have $\prod_{i=1}^{K} \frac{\mu_i}{\mu_i+d_i} \approx e^{-48\times d_0}$. For instance, by assuming that the duration of each repeated compartments is the same for the ODE model (*i.e.*, $\mu_i = \mu_0$, for all $i = 1, \cdots, K$), equality (10) gives $K/\mu_0 = 48$ such that

$$\prod_{i=1}^{K} \frac{\mu_i}{\mu_i + d_i} = (1 + d_0/\mu_0)^{-K} = \exp\left[-K \ln\left(1 + \frac{48 d_0}{K}\right)\right] \approx \exp(-48 d_0) \text{ if } K \gg 1.$$

3.3 Fitting the model parameters with data

The model presented above is solved numerically by using finite volume numerical schemes (implemented with the MatLab Programming Language). The model is then fitted to the data for the time course of gametocytes of the patients. To fit our model, let us observe that most of the parameters are estimated from the literature [4, 21, 29, 41, 42]. Table 1 provides the values we shall use for the fixed parameters. Only three parameters need to be estimated from the data, these are: the proportion of parasitized cells that produce asexual merozoites (α_G), the merozoite initial density (m_0), and the duration of sexual stage ($1/\mu_G$). These parameters are adjusted from the data for each patient by using a least square method. Basically, we find the values which minimize the difference between the ODE model prediction gametocyte density and the observed data by using MatLab nonlinear least-squares solver *lsqcurvefit*. Those optimal parameters for the ODE model are then used to run the PDE model. The superposition of the data and gametocyte density output of the mathematical models are presented in Fig. 3, while the estimated parameter values for each patient are given in Table S1.

3.4 Comparison of ODE and PDE model outputs

We have presented two modelling frameworks to properly model the within-host infection of malaria. Within this context, we compare a classical model based on ordinary differential equations (ODE) with a model based on partial differential equations (PDE). Our first observation is on the parameterisation of both models. More precisely, a good description of the rupture of pRBC requires at least one additional parameter K for the repeated compartments, see (3) versus (4). Such parameter K is necessary to capture the delay in the production or quantification of gametocytes imposed by the development of parasites within RBCs for each infection cycle. This delay in gametocytes production is nicely highlighted by the PDE model formulation (Fig. 3). Trough a "linear chain trick" formulation, it is then possible to find the number K of repeated compartments such that the ODE model can slow down the production dynamics of gametocytes. Indeed, by assuming that the duration of each repeated compartments is the same, we can find K

such that both models perform quite similarly in terms of goodness-of-fit for gametocyte production when the initial production of gametocytes is very slow and hard to find with early sampling, as a consequence of low infection densities and small fractions of pRBCs making gametocytes (Fig. 3, Patient-G299, S1050). However, when the initial parasites load m_0 is relatively high, the PDE model outperforms the K-compartments ODEs which overestimate parasite densities (Fig. 3, Patient-G161, G104). Importantly, the number of compartments for the goodness-of-fit of the ODE model is quite variable across individuals such that the K-compartments ODEs model is definitely less robust compared to the PDE model (Fig. 3). Indeed, while a few number of compartments are necessary for the goodness-of-fit in some configurations (*e.g.*, $K = 6$ for patient G-104, Fig. 3), more compartments are necessary for other configurations (*e.g.*, $K = 16$ for patient G-299, Fig. S1).

According to the infection dynamics, our comparative results show that the PDE model and the K-compartments ODE model (only with $K = 1$) reproduced, at least qualitatively, the true dynamics of malaria infection parasitemia. Indeed, although we do not have parasitemia real data for patients considered here, but in a qualitative comparison to some studies (*e.g.*, [13]), the dynamics of both models (with $K = 1$ for the K-compartments ODE) seem to mimic qualitatively the parasitemia dynamics (Fig. 4). However, the PDE model parasitemia prediction is generally overestimated by the ODE model predictions (Fig. 4). Moreover, when $K \geq 2$, the K-compartments ODE model fails in reproducing realistic parasitemia which is indeed widely underestimated (Fig. 4). As stated previously, one reason for such underestimated parasitemia is that the maturation probabilities D_i,s are very low as K increases (Fig. 2B-D). Finally, even though the K-compartments ODE model (with $K = 1$) qualitatively mimics better realistic dynamics of the malaria infection (including at least the gametocyte and parasitemia dynamics as proxy), this latter model is nevertheless outperformed by the PDE model, particularly early on in infections, where ODE wildly overestimate parasite densities.

3.5 Relationship between parasitemia and gametocyte density

Our mathematical model has been fitted to the available data for each patient under consideration, which consists of gametocyte densities over time. We now use the output of this mathematical model to recover the time course of parasitemia, defined as the proportion of all infected RBC among the total number of RBC, see (9). The time course of parasitemia, $P(t)$, computed from our model are presented in Fig. 5 for each patient together with the fitted gametocyte trajectories. As is observed for each patient, the relationship between these curves exhibits two different regimes. During some period of time $[2, T_0]$, the two curves are increasing with rather similar shape up to a time shift (of length 2 days). This means that, in this increasing regime, the gametocyte density at time t depends on the parasitemia at time $t-2$, a delay which reflects the life cycle of the parasites inside the RBCs. After this period of increasing parasitemia and gametocyte density, namely after time T_0, both curves are decreasing and the shapes seem to depend upon the specific patient considered. To make these comments more quantitative, we introduce the following formula from an estimation of the gametocyte density $G(t)$ from

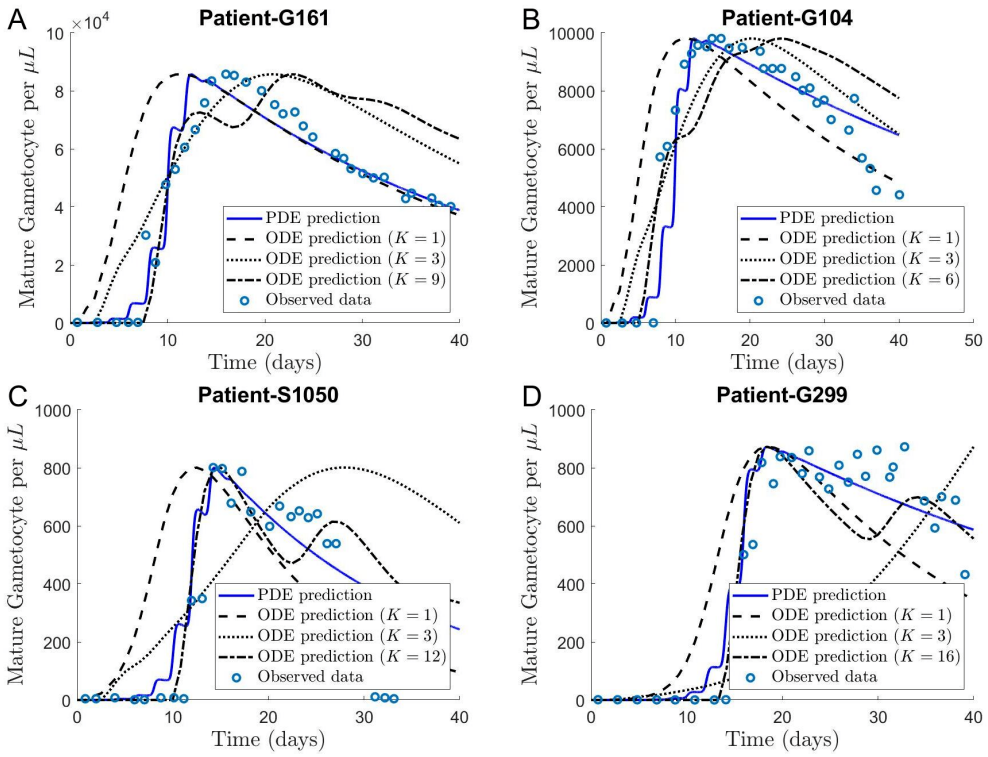

Figure 3: Comparison with data and mathematical model output for gametocyte density for patients G161, G104, S1050 and G299. Comparison for other patients is provided by Figure S1.

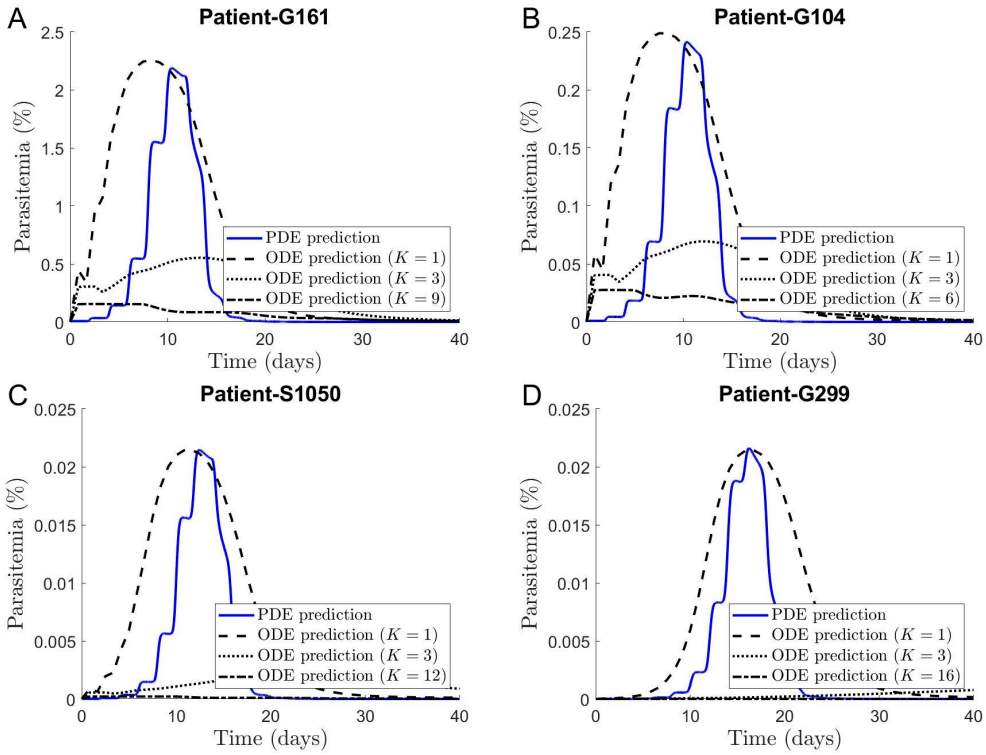

Figure 4: The time course of parasitemia (in percentage) for patients G161, G104, S1050 and G299. Other patients are provided by Figure S2.

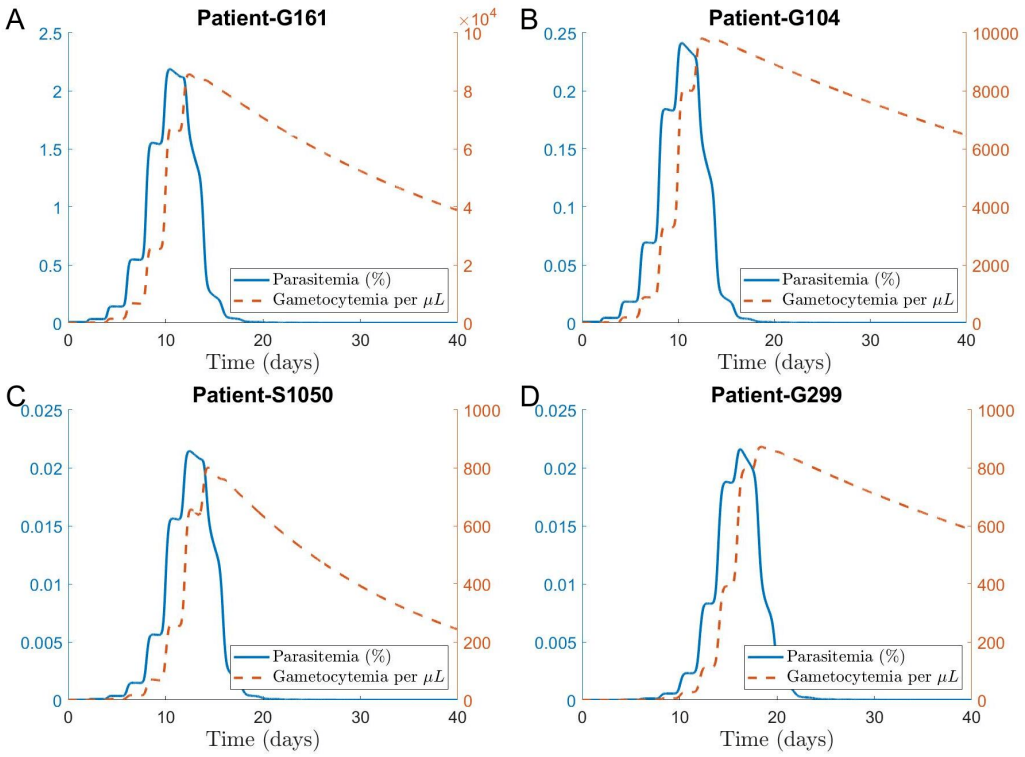

Figure 5: The time course of parasitemia (in percentage) and gametocyte density computed from the PDE model for patients G161, G104, S1050 and G299. Other patients are provided by Figure S3.

the parasitemia $P(t)$:

$$G(t) = \begin{cases} k_1 P(t-2)^{\theta_1} & \text{if } 2 \leq t \leq T_0 \text{ days,} \\ k_2 P(t)^{\theta_2} & \text{if } T_0 \leq t \leq 30, \end{cases} \tag{12}$$

where k_1, k_2, θ_1 and T_0 are four positive parameters while θ_2 is a negative parameter. Let us mention that this 2 days delay between gametocyte density and parasitemia should not to be confused, for example, with the time to distinguish the mature gametocytes via microscopy. Such time is more longer than 2 days and can be well captured by the PDE model in most cases, or by the K-compartments ODE model in some configurations (Fig. 3). While there is a precise biological relationship between parasitemia and gametocytes density at some point in the future, here we seek a robust statistical relationship and so the delay need not match with, *e.g.*, gametocyte maturation time.

To determine the unknown parameters k_1, k_2, θ_1, θ_2 and the changing time T_0 for each patient, we perform a least square analysis. More specifically, we adjust these parameters through a logarithmic scale, that is, through the following formula

$$\log_{10} G(t) = \begin{cases} \log_{10} k_1 + \theta_1 \log_{10} P(t-2) & \text{if } 2 \leq t \leq T_0, \\ \log_{10} k_2 + \theta_2 \log_{10} P(t) & \text{if } T_0 < t \leq 30. \end{cases}$$

To be more precise, our analysis couples the estimate for the time parameter T_0, at which the above formula is changing formulation, together with two linear regressions on each part of the graph. We find that parameters k_1, k_2, θ_1 and T_0 are remarkably robust with respect to individuals while θ_2 depends upon each individual. The results of this analysis as well as the estimated parameters are presented in Fig. S4 and summarized by Table S2 for each patient. The quality of the fit is quantified using the coefficient of determination R^2 (for linear regression). It is computed for each patient and for the two regimes independently. This adjustment metric is computed using the sample of points induced by the time discretization of the partial differential equation model. For our four cases, this coefficient of determination R^2 is approximately 0.99 in the first part of the curve and even closer to one in the second part of the graph.

Coming back to the adjusted parameters described in Table S2, one may observe that the four parameters k_1, k_2, θ_1 and T_0 have robust values with respect to patients while the parameter θ_2 depends on the patient. Using the average values of the adjusted parameters on the set of malariatherapy data, we derive the following clinical formula:

$$G(t) = \begin{cases} 3.843 \times 10^7 \cdot P(t-2)^{+1.0304} & \text{if } 2 < t \leq \overline{T}_0 \text{ days,} \\ 2.981 \times 10^9 \cdot P(t)^{-0.0470} & \text{if } \overline{T}_0 \leq t \leq 30 \text{ days,} \end{cases} \tag{13}$$

with $\overline{T}_0 = 14.5636 \pm 0.0064$ days. The relative error for (13) is such that $\left|\frac{\Delta G}{G}\right|^2 \leq 2.3884 \times 10^{-4} + 1.0617 \left|\frac{\Delta P}{P}\right|^2$, where $\left|\frac{\Delta P}{P}\right|$ is the relative error on the measurement of parasitemia. Therefore, if $\left|\frac{\Delta P}{P}\right| \leq 5\%$, then $\left|\frac{\Delta G}{G}\right| < 5.38\%$. From practical point of view, notice that formula (13) can be really useful to estimate the gametocyte density from the parasitemia measurement without necessarily using the quite 'complex' mathematical model described in this note.

4 Discussion

Many models of within-host malaria infection dynamics have been formulated since the pioneer work of Anderson *el al.* [4] in 1989. These models are based on dynamical systems, with standard approaches ranging from ordinary differential equations (ODEs), to delay differential equations (DDEs) or partial differential equations (PDEs). Most ODE model formulations [25, 28–30, 36, 44, 45] assume an exponential process to describe the rate of pRBCs rupture and therefore fail to capture realistic lifetimes of the pRBCs. This issue is somewhat corrected when the development of parasites within RBCs and rupture of pRBCs are modeled either by a set of K-compartments ODEs [25, 32, 48, 55], or DDEs [11, 23, 30, 34]. Other approaches are the use of PDEs to track the infection history of a pRBC [5, 16, 17, 35]. Using gametocyte production, parasitemia (the proportion of all infected RBC among the total number of RBC) as a proxy variables and malariatherapy data, we found that a PDE model outperforms the K-compartments ODEs in terms of robustness in representing the observed within-host malaria dynamics. Taking K repeated compartments for the ODE model is useful to slow down gametocyte production due to the delay imposed by the parasite development within a RBC, the number of K compartments for the goodness-of-fit of the ODE model is quite variable across individuals. Furthermore, both models perform quite similarly in terms of goodness-of-fit for gametocyte production when the initial production of gametocytes is very slow and hard to find with early sampling. However, when the initial parasites load is relatively high, the PDE model outperforms the K-compartments ODEs which overestimate parasite densities during the first days of infection, approximately the first two weeks.

While a sufficiently high number K of repeated compartments in the ODE model is useful to slow down the initial production of gametocytes (Fig. 3), the predicted parasitemia seems to be unrealistic when $K \geq 2$ (Fig. 4). Consequently, in view of the within-host malaria dynamics (including at least the gametocyte and parasitemia dynamics as proxy), the K-compartements model (with $K = 1$) seems to give a better result compared to cases where $K \geq 2$. This is mainly due to the fact that the ODE model with repeated K compartments imposes short parasite's maturation within a RBC when K increases. Conversely, the PDE model allows the parasite to completely mature within a RBC before the pRBC's rupture. Furthermore, there are major differences in the parasitemia levels, but not in the gametocytes (Fig. 3 and 4), between the K-compartments ODE and PDE model formulations. Such a difference is explained by the fact that the parasitemia is calculated relatively to the total number of RBCs (Eq. 9), such that underestimating the number of pRBCs will greatly impact gametocyte levels.

Not least, the PDE model highlights a strong qualitative connection between gametocyte density and parasitemia which is difficult to capture by the K-compartments ODEs model. From a practical point of view, such a relation given by (13) can be really useful to estimate the gametocyte density from the parasitemia measurement without necessarily using the quite 'complex' mathematical model described in this note.

Here, immune-mediated parasite killing is only considered for merozoites. This choice for immunity targeting merozoites, rather than parasitized red blood cells is mostly because it is a lot easier with our PDE model formulation, particularly in terms of parameterization. However, in some studies, *e.g.* [18], parasite levels are not distinguished by merozoite and parasitized red blood cells, such that immunity is acting against merozoite and parasitized red blood cells. Also note that, while there is evidence that the mature

live gametocytes evade the immune response clearance pathway, immune-mediated parasite killing of immature gametocytes has been shown in some studies [7]. Finally, taking the best fit parameters and then altering immunity parameters between their minimum, median, and maximum values estimated in [18] has very little impact on the model outputs, namely, parasitemia and gametocytes density (figures not shown). However, this can be explain by the fact that (i) merozoites are only short lived and (ii) the relatively short-term validation of the model presented here.

Reducing infections in mosquitoes—vectors of *Plasmodium* parasites—is a crucial component of global efforts to control and eliminate malaria [3]. Because a strong correlation exits between the gametocyte density within a host and infectivity of mosquitoes [9, 14, 15, 27], progress towards this goal would be bolstered by quantifying gametocytes and identifying highly infectious hosts [10, 52, 53]. On the other hand, parasitemia is easily quantified by light microscopy and therefore is more technically accessible, particularly in regions where malaria is endemic. Therefore, quantifying the relationship between the gametocyte density and parasitemia is of great interest to define more simple tools for the prediction of mosquito infection. The results presented in this note provide one such tool.

From a public health or population dynamics point of view, the time course of the disease at the between-host level is strongly related to the basic reproduction number (also denoted here by $\mathcal{R}_0$). At the between-host level, the $\mathcal{R}_0$ is defined as the number of secondary infections from a single infected individual introduced in a fully susceptible population. This important metric can be estimated from real data but also using mathematical models. The simplest (deterministic) mathematical model reads as the Ross system of equations from which one can compute this threshold number $\mathcal{R}_0$ as follows:

$$\text{Between-host} \left\| \mathcal{R}_0 = \mathcal{R}_0^{VH} \times \mathcal{R}_0^{HV} \text{ with } \begin{cases} \mathcal{R}_0^{VH} = abd_M, \\ \mathcal{R}_0^{HV} = macd_H. \end{cases} \right.$$

Note that the above $\mathcal{R}_0$ is for between-host malaria dynamics and is not for the within-host models presented here. In the above formula of $\mathcal{R}_0$, m represents the number of mosquitoes per person, a denotes the mosquito biting rate, b and c denote the per bite transmission probability respectively from mosquito to human and from human to mosquito, while d_H and d_M correspond respectively to the human recovery and the mosquito death rates. Although more ingredients can been included into the mathematical model, leading to different formulations for $\mathcal{R}_0$, the above expression contains the main important parameters [38, 39, 50]. Parameters b and c serve as the link between within- and between-host dynamics, since the transmission rates from (to) a host will depend on the dynamics of what is happening within that host (vector). Furthermore, there is a clear relationship between gametocyte density (G) and the transmission probability per bite from human to mosquito (c) [8, 9, 14, 15, 20, 33, 51]. From a practical point of view, the parameter c is difficult to estimate in a relevant way. Indeed, an efficient measurement of c requires a good measure of the gametocyte density which is quite difficult to obtain in practice. Indeed, while we can get either gametocytes or parasitemia from microscopy, but with gametocytes tending to be at lower densities (sometimes orders of magnitude lower), there is a detectability issue. Thus, a simple way to estimate the gametocyte density will help to infer the parameter c. Thanks to formula (12) proposed here, we then have robust relationships between parasitemia (easier to measure) and gametocyte density, at least during the first days of infection (approximately the first two weeks).

Overall, the proposed model for the dynamics of gametocytes is probably valid for the first asexual wave which last approximately 40 days for each patient in this malariatherapy dataset. This relatively short-term validation is enough for the aim of the current study. However, for the long-term gametocyte dynamics, we need to bring more complexity in the model proposed here. Indeed, the conversion probability of asexual parasites to circulating gametocytes (α_G) should be considered to vary among successive waves of asexual parasitaemia to tackle such issue of the long-term gametocyte dynamics [21], particularly since smear-positive asymptomatic malaria infections detectable by microscopy are an important gametocytes reservoir and often persist for months [37].

The robustness of the model proposed here, especially the formula linking parasitaemia and gametocyte density, is only guaranteed during the first two weeks after infection. Beyond this time, this estimate is highly variable from one patient to another. This variability is explained, at least in part, by the variability of the duration of sexual stage ($1/\mu_G$) which governs the decrease in gametocyte density (Table S1). One interpretation of the variation in this parameter is that there exists variation in how well individuals clear gametocytes or kill them through immune responses [19, 37]. Less variability is expected at the beginning of infection, where the whole system is less constrained by immunity. This is likely to be true for the malariatherapy patient data presented here, since hosts were initially naive. However in high transmission settings, acquired immunity—particularly in older hosts—may obscure the relationship between early gametocyte and asexual parasite densities our work has revealed. Furthermore, fine scale, longitudinal data could assess the applicability of this relationship across settings and age groups, although such data is understandably difficult to obtain.

Finally, while our work reveals a simple tool for linking aspects of the early dynamics of malaria infections, it also offers specific suggestions for how best to mathematically describe those infection dynamics more broadly. Both PDE and K-compartments ODE models have been adopted to capture the subtleties of malaria parasite life cycles in blood-stage infections [35]. Our work provides more evidence that, among those choices, PDE models offer clear advantages.

Table 1: Fixed model parameters

Parameters	Description (unit)	Values	References
Λ_0	Production rate of RBC (RBC/h/ml)	1.73×10^6	[4, 42]
$1/\mu_{r\to m}$	Duration of the RBC reticulocyte stage (h)	36	[41]
$1/\mu_{m\to s}$	Duration of the RBC mature stage (day)	116.5	[41]
$1/\mu_{s\to d}$	Duration of the RBC senescent stage (h)	48	[41]
β	Infection rate of uRBC (RBC/ml/day)	6.27×10^{-10}	[4]
d_0	Natural death rate of uRBC (RBC.day^{-1})	0.00833	[4]
μ_m	Decay rates of malaria parasites (RBC.day^{-1})	48	[29]
r	Merozoites multiplication factor (dimensionless)	16	[4]
α_G	Proportion of sexual merozoites (dimensionless)	0.05	[42]
S_I^*	Innate IR density for 50% of parasite killing (cells.μl^{-1})	2,755	[18]
S_A^*	Adaptive IR density for 50% of parasite killing (cells.μl^{-1})	20.4	[18]
Δ_0	Delay required by adaptive IR to be effective (day)	16	[18]

Table 2: Initial values for the model

Variables	Description	Initial Values
$R_r(0)$	Population of reticulocytes RBC	62×10^6 RBC.ml^{-1}
$R_m(0)$	Population of mature RBC	4.85×10^9 RBC.ml^{-1}
$R_s(0)$	Population of senescent RBC	83×10^6 RBC.ml^{-1}
$p(0,.)$	Population of pRBC for the PDE model	0 cells.ml^{-1}
p_j	Population of pRBC for the ODE màdel	0 cells.ml^{-1}
$G(0)$	Population of mature gametocyte	0 cells.ml^{-1}
$m(0)$	Population of malaria parasites	variable

Acknowledgements

Authors thank Samuel Alizon, Laurence Ayong, Carole Eboumbou and Christophe Rogier for comments and suggestions to improve the manuscript.

Code availability

The code (with the MatLab Programming Language) used to simulate the model can be accessed through the Zenodo platform at `https://doi.org/10.5281/zenodo.5526271`

References

References

[1] F. B. Agusto, M. C. A. Leite, and M. E. Orive. The transmission dynamics of a within-and between-hosts malaria model. *Ecological Complexity*, 38:31–55, Apr. 2019.

[2] P. Alano and R. Carter. Sexual differentiation in malaria parasites. *Annual Review of Microbiology*, 44(1):429–449, Oct. 1990.

[3] P. L. Alonso, G. Brown, M. Arevalo-Herrera, F. Binka, C. Chitnis, F. Collins, O. K. Doumbo, B. Greenwood, B. F. Hall, M. M. Levine, K. Mendis, R. D. Newman, C. V. Plowe, M. H. Rodríguez, R. Sinden, L. Slutsker, and M. Tanner. A Research Agenda to Underpin Malaria Eradication. *PLOS Medicine*, 8(1):e1000406, Jan. 2011.

[4] R. M. Anderson, R. M. May, and S. Gupta. Non-linear phenomena in host-parasite interactions. *Parasitology*, 99 Suppl:S59–79, 1989.

[5] R. Antia, A. Yates, and J. C. de Roode. The dynamics of acute malaria infections. I. Effect of the parasite's red blood cell preference. *Proceedings of the Royal Society B: Biological Sciences*, 275(1641):1449–1458, June 2008.

[6] L. Bannister and G. Mitchell. The ins, outs and roundabouts of malaria. *Trends in Parasitology*, 19(5):209–213, May 2003.

[7] G. P. Bansal and N. Kumar. Immune Responses in Malaria Transmission. *Current Clinical Microbiology Reports*, 5(1):38–44, Mar. 2018.

[8] T. Bousema, R. R. Dinglasan, I. Morlais, L. C. Gouagna, T. van Warmerdam, P. H. Awono-Ambene, S. Bonnet, M. Diallo, M. Coulibaly, T. Tchuinkam, B. Mulder, G. Targett, C. Drakeley, C. Sutherland, V. Robert, O. Doumbo, Y. Touré, P. M. Graves, W. Roeffen, R. Sauerwein, A. Birkett, E. Locke, M. Morin, Y. Wu, and T. S. Churcher. Mosquito Feeding Assays to Determine the Infectiousness of Naturally Infected Plasmodium falciparum Gametocyte Carriers. *PLOS ONE*, 7(8):e42821, Aug. 2012.

[9] T. Bousema and C. Drakeley. Epidemiology and Infectivity of Plasmodium falciparum and Plasmodium vivax Gametocytes in Relation to Malaria Control and Elimination. *Clinical Microbiology Reviews*, 24(2):377–410, Apr. 2011.

[10] T. Bousema and C. Drakeley. Determinants of Malaria Transmission at the Population Level. *Cold Spring Harbor Perspectives in Medicine*, 7(12), Dec. 2017.

[11] P. Cao, K. A. Collins, S. Zaloumis, T. Wattanakul, J. Tarning, J. A. Simpson, J. McCarthy, and J. M. McCaw. Modeling the dynamics of Plasmodium falciparum gametocytes in humans during malaria infection. *eLife*, 8:e49058, Oct. 2019.

[12] E. Chernin. The Malariatherapy of Neurosyphilis. *The Journal of Parasitology*, 70(5):611–617, 1984.

[13] L. M. Childs and C. O. Buckee. Dissecting the determinants of malaria chronicity: Why within-host models struggle to reproduce infection dynamics. *Journal of the Royal Society, Interface*, 12(104):20141379, Mar. 2015.

[14] T. S. Churcher, T. Bousema, M. Walker, C. Drakeley, P. Schneider, A. L. Ouédraogo, and M.-G. Basáñez. Predicting mosquito infection from Plasmodium falciparum gametocyte density and estimating the reservoir of infection. *eLife*, 2:e00626, May 2013.

[15] W. E. Collins and G. M. Jeffery. A retrospective examination of mosquito infection on humans infected with Plasmodium falciparum. *The American Journal of Tropical Medicine and Hygiene*, 68(3):366–371, Mar. 2003.

[16] D. Cromer, J. Stark, and M. P. Davenport. Low red cell production may protect against severe anemia during a malaria infection—Insights from modeling. *Journal of Theoretical Biology*, 257(4):533–542, Apr. 2009.

[17] R. D. Demasse and A. Ducrot. An Age-Structured Within-Host Model for Multistrain Malaria Infections. *SIAM Journal on Applied Mathematics*, 73(1):572–593, Jan. 2013.

[18] K. Dietz, G. Raddatz, and L. Molineaux. Mathematical model of the first wave of plasmodium falciparum asexual parasitemia in non-immune and vaccinated individuals. *The American Journal of Tropical Medicine and Hygiene*, 75(2_suppl):46–55, Aug. 2006.

[19] D. L. Doolan, C. Dobaño, and J. K. Baird. Acquired Immunity to Malaria. *Clinical Microbiology Reviews*, 22(1):13–36, Jan. 2009.

[20] C. J. Drakeley, I. Secka, S. Correa, B. M. Greenwood, and G. A. Targett. Host haematological factors influencing the transmission of Plasmodium falciparum gametocytes to Anopheles gambiae s.s. mosquitoes. *Tropical medicine & international health: TM & IH*, 4(2):131–138, Feb. 1999.

[21] M. Eichner, H. H. Diebner, L. Molineaux, W. E. Collins, G. M. Jeffery, and K. Dietz. Genesis, sequestration and survival of Plasmodium falciparum gametocytes: Parameter estimates from fitting a model to malariatherapy data. *Transactions of The Royal Society of Tropical Medicine and Hygiene*, 95(5):497–501, Sept. 2001.

[22] Z. Feng, D. Xu, and H. Zhao. Epidemiological models with non-exponentially distributed disease stages and applications to disease control. *Bulletin of Mathematical Biology*, 69(5):1511–1536, July 2007.

[23] L. L. Fonseca and E. O. Voit. Comparison of Mathematical Frameworks for Modeling Erythropoiesis in the Context of Malaria Infection. *Mathematical biosciences*, 270(0 0):224–236, Dec. 2015.

[24] U. Frevert. Sneaking in through the back entrance: The biology of malaria liver stages. *Trends in Parasitology*, 20(9):417–424, Sept. 2004.

[25] M. B. Gravenor and A. L. Lloyd. Reply to: Models for the in-host dynamics of malaria revisited: Errors in some basic models lead to large over-estimates of growth rates. *Parasitology*, 117(5):409–410, Nov. 1998.

[26] M. B. Gravenor, A. L. Lloyd, P. G. Kremsner, M. A. Missinou, M. English, K. Marsh, and D. Kwiatkowski. A Model for Estimating Total Parasite Load in Falciparum Malaria Patients. *Journal of Theoretical Biology*, 217(2):137–148, July 2002.

[27] P. M. Graves, T. R. Burkot, R. Carter, J. A. Cattani, M. Lagog, J. Parker, B. J. Brabin, F. D. Gibson, D. J. Bradley, and M. P. Alpers. Measurement of malarial infectivity of human populations to mosquitoes in the Madang area, Papua New Guinea. *Parasitology*, 96(2):251–263, Apr. 1988.

[28] B. Hellriegel. Modelling the immune response to malaria with ecological concepts: Short-term behaviour against long-term equilibrium. *Proceedings of the Royal Society of London. Series B: Biological Sciences*, 250(1329):249–256, Dec. 1992.

[29] C. Hetzel and R. M. Anderson. The within-host cellular dynamics of bloodstage malaria: Theoretical and experimental studies. *Parasitology*, 113 (Pt 1):25–38, July 1996.

[30] M. B. Hoshen, R. Heinrich, W. D. Stein, and H. Ginsburg. Mathematical modelling of the within-host dynamics of Plasmodium falciparum. *Parasitology*, 121 (Pt 3):227–235, Sept. 2000.

[31] P. J. Hurtado and A. S. Kirosingh. Generalizations of the 'Linear Chain Trick': Incorporating more flexible dwell time distributions into mean field ODE models. *Journal of Mathematical Biology*, 79(5):1831–1883, Oct. 2019.

[32] A. Iggidr, J.-C. Kamgang, G. Sallet, and J.-J. Tewa. Global Analysis of New Malaria Intrahost Models with a Competitive Exclusion Principle. *SIAM Journal on Applied Mathematics*, 67(1):260–278, Jan. 2006.

[33] G. L. Johnston, D. L. Smith, and D. A. Fidock. Malaria's Missing Number: Calculating the Human Component of R0 by a Within-Host Mechanistic Model of Plasmodium falciparum Infection and Transmission. *PLOS Computational Biology*, 9(4):e1003025, Apr. 2013.

[34] D. H. Kerlin and M. L. Gatton. Preferential Invasion by Plasmodium Merozoites and the Self-Regulation of Parasite Burden. *PLOS ONE*, 8(2):e57434, Feb. 2013.

[35] D. S. Khoury, R. Aogo, G. Randriafanomezantsoa-Radohery, J. M. McCaw, J. A. Simpson, J. S. McCarthy, A. Haque, D. Cromer, and M. P. Davenport. Within-host modeling of blood-stage malaria. *Immunological Reviews*, 285(1):168–193, 2018.

[36] Y. Li, S. Ruan, and D. Xiao. The within-host dynamics of malaria infection with immune response. *Mathematical biosciences and engineering: MBE*, 8(4):999–1018, Oct. 2011.

[37] J. T. Lin, D. L. Saunders, and S. R. Meshnick. The role of submicroscopic parasitemia in malaria transmission: What is the evidence? *Trends in Parasitology*, 30(4):183–190, Apr. 2014.

[38] G. Macdonald. The Measurement of Malaria Transmission. *Proceedings of the Royal Society of Medicine*, 48(4):295–302, Apr. 1955.

[39] S. Mandal, R. R. Sarkar, and S. Sinha. Mathematical models of malaria - a review. *Malaria Journal*, 10(1):202, July 2011.

[40] F. E. McKenzie and W. H. Bossert. An integrated model of Plasmodium falciparum dynamics. *Journal of Theoretical Biology*, 232(3):411–426, Feb. 2005.

[41] P. G. McQueen and F. E. McKenzie. Host Control of Malaria Infections: Constraints on Immune and Erythropoeitic Response Kinetics. *PLOS Computational Biology*, 4(8):e1000149, Aug. 2008.

[42] P. G. McQueen, K. C. Williamson, and F. E. McKenzie. Host immune constraints on malaria transmission: Insights from population biology of within-host parasites. *Malaria Journal*, 12(1):206, June 2013.

[43] L. H. Miller, H. C. Ackerman, X.-z. Su, and T. E. Wellems. Malaria biology and disease pathogenesis: Insights for new treatments. *Nature medicine*, 19(2):156–167, Feb. 2013.

[44] J. L. Mitchell and T. W. Carr. Oscillations in an Intra-host Model of Plasmodium Falciparum Malaria Due to Cross-reactive Immune Response. *Bulletin of Mathematical Biology*, 72(3):590–610, Apr. 2010.

[45] L. Molineaux and K. Dietz. Review of intra-host models of malaria. *Parassitologia*, 41(1-3):221–231, Sept. 1999.

[46] R. E. L. Paul, F. Ariey, and V. Robert. The evolutionary ecology of Plasmodium. *Ecology Letters*, 6(9):866–880, 2003.

[47] R. C. Russell, D. Otranto, and R. L. Wall. *The Encyclopedia of Medical and Veterinary Entomology*. CABI, 2013.

[48] S. Saralamba, W. Pan-Ngum, R. J. Maude, S. J. Lee, J. Tarning, N. Lindegårdh, K. Chotivanich, F. Nosten, N. P. J. Day, D. Socheat, N. J. White, A. M. Dondorp, and L. J. White. Intrahost modeling of artemisinin resistance in Plasmodium falciparum. *Proceedings of the National Academy of Sciences*, 108(1):397–402, Jan. 2011.

[49] A. Saul. Models for the in-host dynamics of malaria revisited: Errors in some basic models lead to large over-estimates of growth rates. *Parasitology*, 117(5):405–407, Nov. 1998.

[50] D. L. Smith, K. E. Battle, S. I. Hay, C. M. Barker, T. W. Scott, and F. E. McKenzie. Ross, macdonald, and a theory for the dynamics and control of mosquito-transmitted pathogens. *PLoS pathogens*, 8(4):e1002588, 2012.

[51] K. Stepniewska, R. N. Price, C. J. Sutherland, C. J. Drakeley, L. von Seidlein, F. Nosten, and N. J. White. Plasmodium falciparum gametocyte dynamics in areas of different malaria endemicity. *Malaria Journal*, 7(1):249, Dec. 2008.

[52] W. Stone, B. P. Gonçalves, T. Bousema, and C. Drakeley. Assessing the infectious reservoir of falciparum malaria: Past and future. *Trends in Parasitology*, 31(7):287–296, July 2015.

[53] T. m. R. C. P. o. C. t. R. a. M. Transmission. malERA: An updated research agenda for characterising the reservoir and measuring transmission in malaria elimination and eradication. *PLOS Medicine*, 14(11):e1002452, Nov. 2017.

[54] World Health Organization. *World Malaria Report 2019.* World Health Organization, S.l., 2019.

[55] S. Zaloumis, A. Humberstone, S. A. Charman, R. N. Price, J. Moehrle, J. Gamo-Benito, J. McCaw, K. M. Jamsen, K. Smith, and J. A. Simpson. Assessing the utility of an anti-malarial pharmacokinetic-pharmacodynamic model for aiding drug clinical development. *Malaria Journal*, 11(1):303, Aug. 2012.

A Explicit estimation of the total number of pRBCs

Let us set $N(t) = \beta m(t) \sum_{j=r,m,s} \gamma_j R_j(t)$, the number of newly pRBCs at time t. Since $p_1(0) = 0$, we have by System (4),

$$\begin{cases} p_1(t) = \displaystyle\int_0^t N(\sigma) e^{-(\mu_1+d_1)(t-\sigma)} d\sigma, \\ p_i(t) = \displaystyle\int_0^t \mu_{i-1} p_{i-1}(\sigma) e^{-(\mu_i+d_i)(t-\sigma)} d\sigma, \quad \text{for } i = 2, \dots, K. \end{cases} \tag{A.1}$$

Next, assuming that the duration of each repeated compartments is the same (*i.e.*, $\mu_i = \mu_0$, for all $i = 1, \cdots, K$), by (10), we have $\mu_i = K/48$, for all $i = 1, \cdots, K$; and (A.1) rewrites

$$\begin{cases} p_1(t) = \displaystyle\int_0^t N(\sigma) e^{-(\frac{K}{48}+d_1)(t-\sigma)} d\sigma, \\ p_i(t) = \displaystyle\int_0^t \mu_{i-1} p_{i-1}(\sigma) e^{-(\frac{K}{48}+d_i)(t-\sigma)} d\sigma, \quad \text{for } i = 2, \dots, K. \end{cases}$$

Consequently, the total number of pRBCs $\sum_{i=1}^K p_i(t)$ –counted by the ODE model– at time t will lead to a wide underestimation of the development of the overall parasite dynamics for large values of K. That is because the maturation probability in the i-stage after a hours of infection, $D_i(a) = e^{-(\frac{K}{48}+d_i)a}$, will be very low as K and a increase. More precisely, when RBCs natural mortality d_i is neglected, such probability is less than 0.4 as soon as $aK/48 > 1$, *i.e.* $a > 48/K$ hours.

The above problem –*i.e.* the underestimation of the development of parasite dynamics– does not hold with the PDE model formulation. Indeed, since $p(0, \cdot) \equiv 0$, by solving System (3) along the characteristics, we have

$$p(t,a) = \begin{cases} 0, \quad \text{for } t < a, \\ N(t-a) e^{-\int_0^a (\mu(\sigma)+d_0) d\sigma}, \quad \text{for } t \geq a, \end{cases} \tag{A.2}$$

Therefore, the total number of pRBCs –counted by the PDE model– at time t is given by

$$\begin{aligned} \int_0^\infty p(t,a) da &= \int_0^t N(t-a) e^{-\int_0^a (\mu(\sigma)+d_0) d\sigma} da \\ &= \begin{cases} \displaystyle\int_0^t N(a) e^{-d_0(t-a)} da, \quad \text{for } t < 48, \\ \displaystyle\int_0^{48} N(a) e^{-d_0(t-a)} da + \int_0^{t-48} N(a) e^{-d_0(t-a)} e^{-\bar{\mu}(t-a-48)} da, \quad \text{for } t > 48. \end{cases} \end{aligned}$$

B Supplementary figures

Figure S1: Comparison with data and mathematical model output for gametocyte density for other patients.

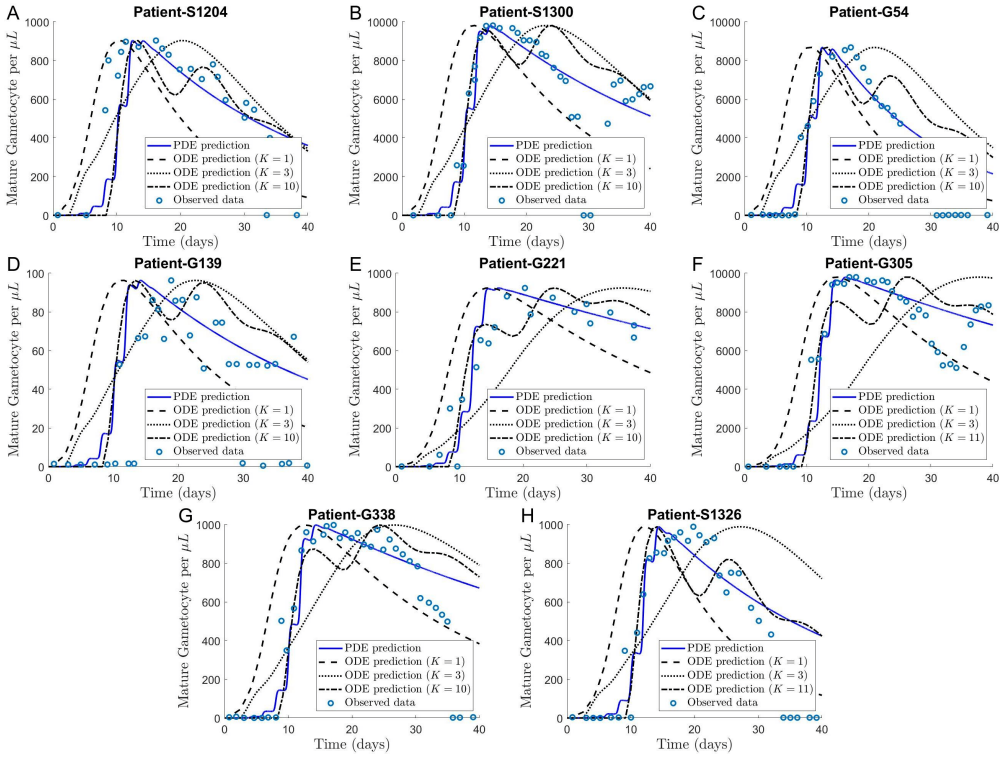

Figure S2: The time evolution of parasitemia (in percentage) density for other patients.

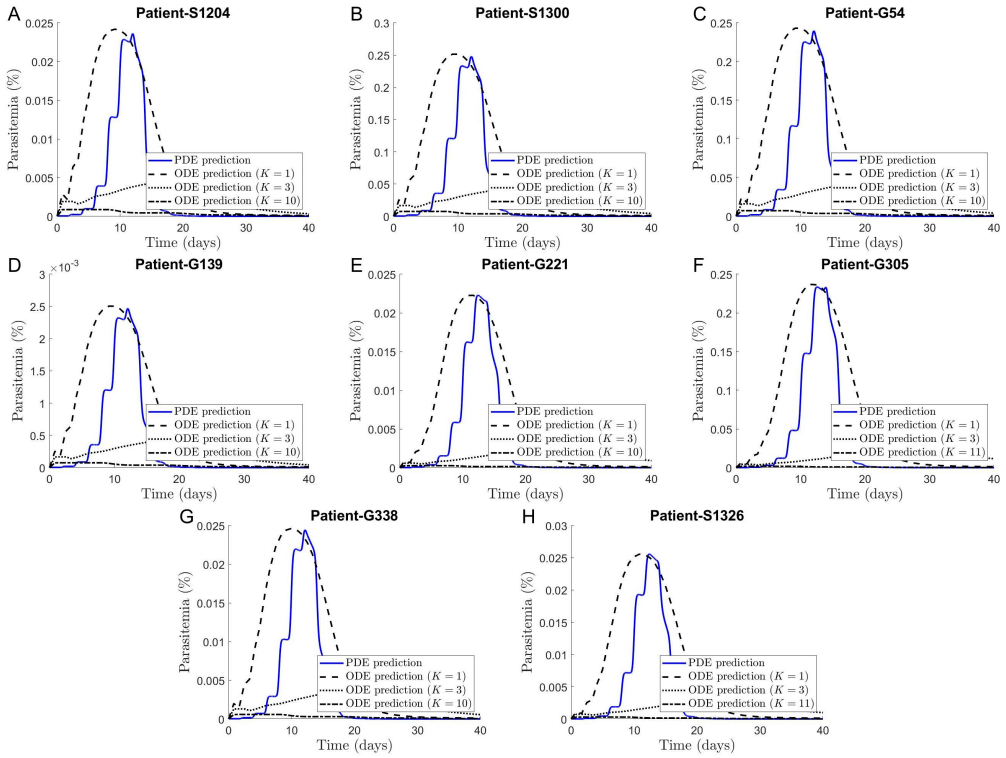

Figure S3: The time evolution of parasitemia (in percentage) and gametocyte density curves computed from the PDE model for other patients.

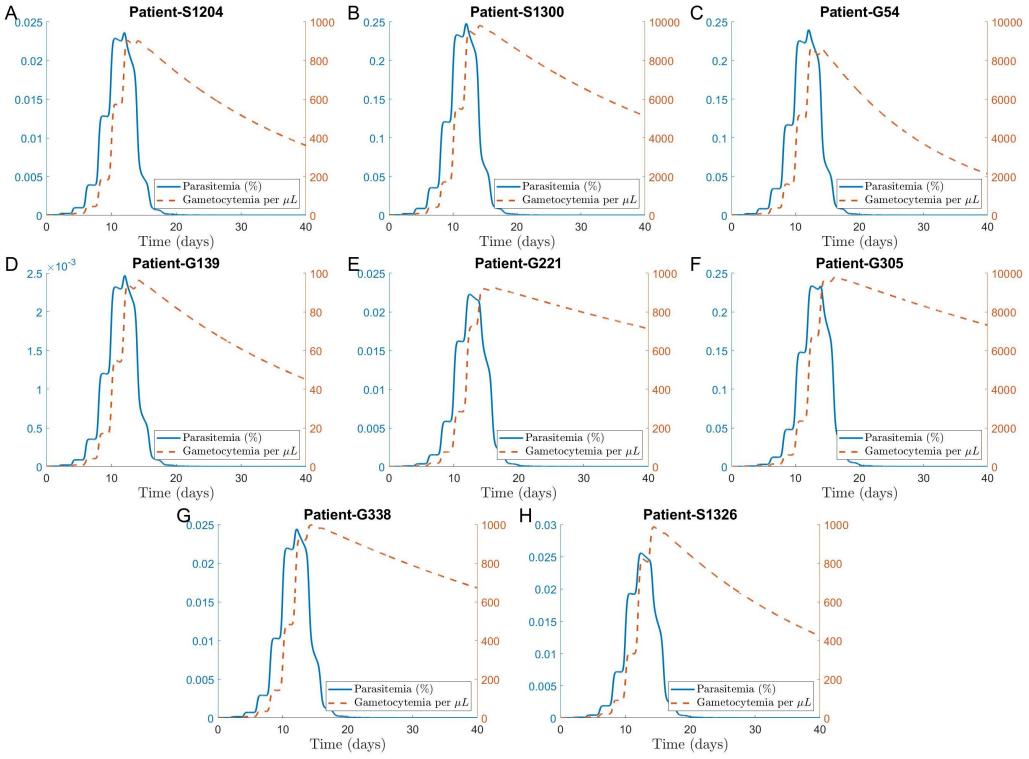

Figure S4: Comparison between model prediction and the linear regression based on formula (12)

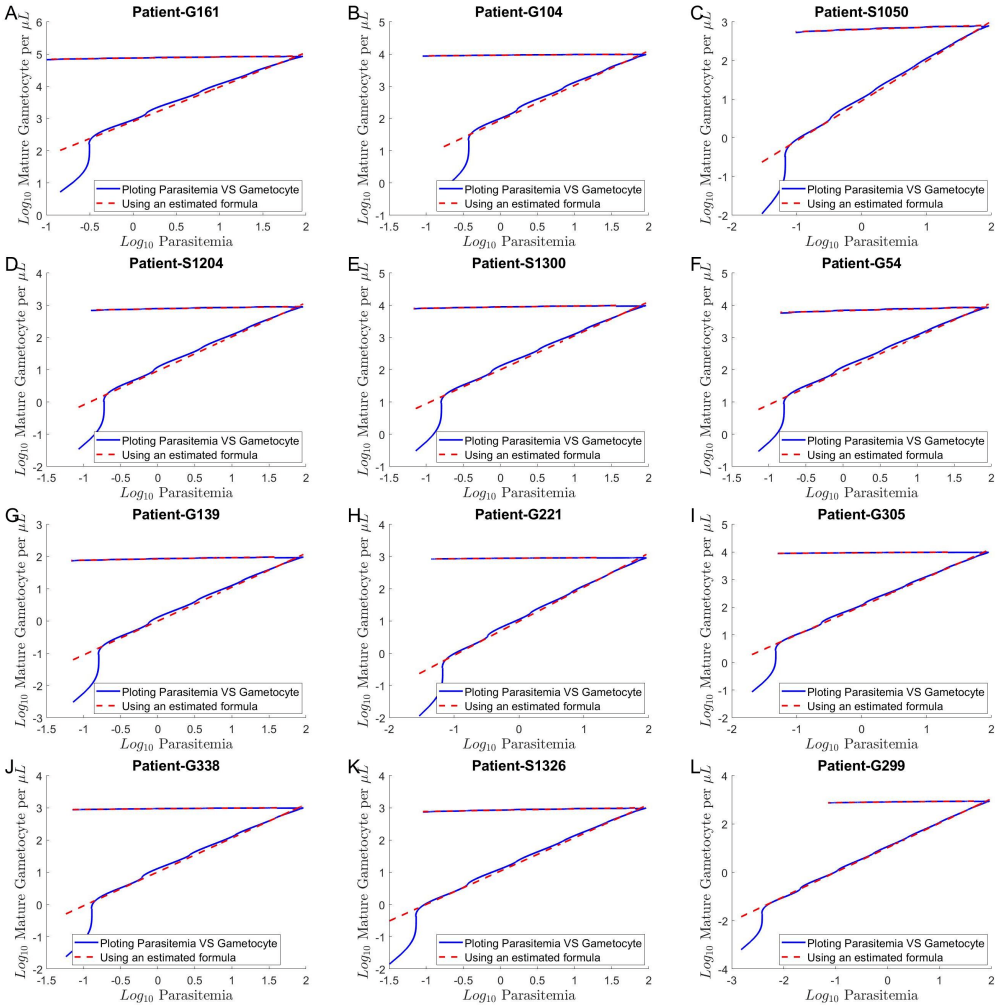

C Supplementary tables

Table S1: Patient-specific parameters estimated from the data

	G54	G221	S1050	S1204	S1300	G104
$\mu_G(\times 10^{-3})$	2.27	0.4632	1.99	1.5	1.07	0.667
$\alpha_G(\times 10^{-8})$	13.02	1.206	1.161	1.289	13.47	13.02
$m_0(\times 10^7)$	2.5	1	1	2.97	2.5	6
	G139	G161	G305	G338	G299	S1326
$\mu_G(\times 10^{-3})$	1.25	1.25	0.526	0.667	0.80	1.43
$\alpha_G(\times 10^{-8})$	0.134	118.57	12.84	1.321	1.1682	1.382
$m_0(\times 10^7)$	2.5	5	0.7	2	0.05	1.1

Table S2: Estimated parameters for the shape (12)

	G221	G54	S1050	S1204
$\log_{10}(k_1)$	2.9586 ± 0.0037	2.9326 ± 0.0039	2.9520 ± 0.0037	2.9502 ± 0.0037
θ_1	1.0321 ± 0.0028	1.0312 ± 0.0030	1.0315 ± 0.0029	1.0315 ± 0.0028
$\log_{10}(k_2)$	2.9437 ± 0.0002	3.8802 ± 0.0005	2.9101 ± 0.0004	2.9148 ± 0.0003
θ_2	-0.0141 ± 0.0004	-0.0477 ± 0.0005	-0.0336 ± 0.0005	-0.0280 ± 0.0003
T_0(days)	14.7125 ± 0.0075	13.2917 ± 0.0083	14.4958 ± 0.0083	13.4666 ± 0.0025
	S1300	G104	G139	G161
$\log_{10}(k_1)$	2.9861 ± 0.0037	2.9821 ± 0.0041	2.8024 ± 0.0037	2.9272 ± 0.0039
θ_1	1.0315 ± 0.0028	1.0304 ± 0.0031	1.0315 ± 0.0028	1.0312 ± 0.0029
$\log_{10}(k_2)$	3.9442 ± 0.0003	3.9663 ± 0.0002	1.9360 ± 0.0003	4.8774 ± 0.0002
θ_2	-0.0336 ± 0.0003	-0.0170 ± 0.0002	-0.0336 ± 0.0003	-0.0214 ± 0.0003
T_0(days)	14.5375 ± 0.0075	13.2625 ± 0.0083	14.5625 ± 0.0083	13.3875 ± 0.0025
	G299	G305	G338	S1326
$\log_{10}(k_1)$	2.9712 ± 0.0034	2.9854 ± 0.0037	2.9897 ± 0.0041	2.9893 ± 0.0037
θ_1	1.0301 ± 0.0027	1.0315 ± 0.0028	1.0304 ± 0.0031	1.0315 ± 0.0028
$\log_{10}(k_2)$	2.9063 ± 0.0003	3.9607 ± 0.0001	2.9739 ± 0.0002	2.9474 ± 0.0003
θ_2	-0.0203 ± 0.0003	-0.0188 ± 0.0002	-0.0170 ± 0.0002	-0.0336 ± 0.0003
T_0(days)	20.0083 ± 0.0075	14.6917 ± 0.0083	14.2625 ± 0.0083	14.5458 ± 0.0025